Scientific Research Publishing

Engineering, 2025, 17(5), 289-314
https://www.scirp.org/journal/eng
ISSN Online: 1947-394X
ISSN Print: 1947-3931

LCL Filter and Dampers for a Three-Phase, Two-Level Inverter with Six-Pulse Control

Kouakou Fernand Koffi[1*], Bi Irié Cyrille Dje[2], N'Guessan Kouamé Norbert[1], Georges Loum[1*], Olivier Asseu[1,2]

[1]INPHB, EDP-STI, Côte d'Ivoire
[2]LASTIC, ESATIC, Abidjan, Côte d'Ivoire
Email: *kouakou_kouakou@ymail.com, iriecyrille.djebi@esatic.edu.ci, norbert.nguessan@inphb.ci, *georges.loum@inphb.ci, oasseu@yahoo.fr

How to cite this paper: Koffi, K.F., Dje, B.I.C., Norbert, N.K., Loum, G. and Asseu, O. (2025) LCL Filter and Dampers for a Three-Phase, Two-Level Inverter with Six-Pulse Control. *Engineering*, **17**, 289-314.
https://doi.org/10.4236/eng.2025.175018

Received: April 29, 2025
Accepted: May 28, 2025
Published: May 31, 2025

Abstract

In this article, the LCL filter used for the three-phase two-level inverter with six-pulse control is designed from the components of the LC filter by means of a coefficient k varying between 0 and 1. The coefficient k is used to determine the values of the inductances of the LCL filter in relation to the inductance of the LC filter. The capacitor capacity of the LCL filter is identical to that of the LC filter. To obtain the RMS voltage and current of the load, a method based on measuring the error of the RMS voltage and current of the load is proposed. This approach, applied to the three-phase, two-level inverter with 180˚ full-wave control, enables us to reduce the value of the LCL filter inductance. Satisfactory results are obtained by simulation on MATLAB-Simulink software and compared with the LCL filter results.

Keywords

LC Filter, LCL Filter, Three-Phase Two-Level Inverter with Six-Pulse Control, Damper, THD, MATLAB-Simulink

1. Introduction

The rapid expansion of renewable energies such as photovoltaic solar power raises questions about the quality of the alternative energy sent to rural localities (electrical loads). This is because a photovoltaic solar power plant produces DC energy, which is converted by a two-stage three-phase inverter. After conversion to AC, the voltage and current signals do not comply with the IEEE 519-2014 standard [1]. Especially if the three-phase two-level inverter has six-pulse control, the voltage THD is over 34% and the current THD depends on the nature of the electrical

load. The SPWM-controlled inverter has a voltage THD close to 100%, but the current THD is around 10%. In all cases, AC filters must be used to reduce voltage and current THD. But there is also a need to have an RMS voltage and current value for a load at a low error rate. Hence, the use of dampers in the LCL filter.

Six-pulse control is specific to three-phase, two-level DC/AC converters. It is stable and is performed at low frequency, unlike SPWM control. It has many advantages: higher efficiency than SPWM control. In 180˚ control, the use of any type of semiconductor (thyristor, bipolar transistor, MOSFET and IGBT transistor) is permitted, unlike SPWM control, which does not use thyristors and bipolar transistors, as they are unable to switch at high frequencies due to losses [2]-[5].

To be used to supply rural communities, the energy available at the output of the 180˚-controlled two-level inverter needs to be filtered. Passive filters can solve this problem. There are several types of AC filters with different topologies: L, LC, LCL, LLCL with their derivatives and dampers [6]-[8]. For reasons of efficiency, size, cost and reliability, weight and volume, the use of AC filters is reduced to LC and LCL topologies [9]-[11].

In the paper [12], we developed a mathematical approach that enabled us to obtain the minimum and maximum values of the inductance and capacitance of the LC filter for the three-phase, two-level inverter with 180˚ full control. These results are used to size the LCL filter.

Our contribution is based on three points:

1) Sizing the LCL filter using the formulas for minimum and maximum values of LC filter inductance and capacitance developed in the paper [12];

2) Sizing the LCL filter dampers;

3) Compare voltage and current THDs for different combinations of minimum and maximum inductances, minimum and maximum capacitor capacities.

The paper is presented as follows: in section II, the system model and problem formulation are carried out; in section III, the formulas for sizing the LC filter of the three-phase two-level 180˚ full control inverter are recalled; in section IV, the determination of the LCL filter expressions by introducing a coefficient k; in section V, the method for sizing the LCL filter dampers; and in section VI, an analysis of the results is made.

2. System Model and Problem Formulation

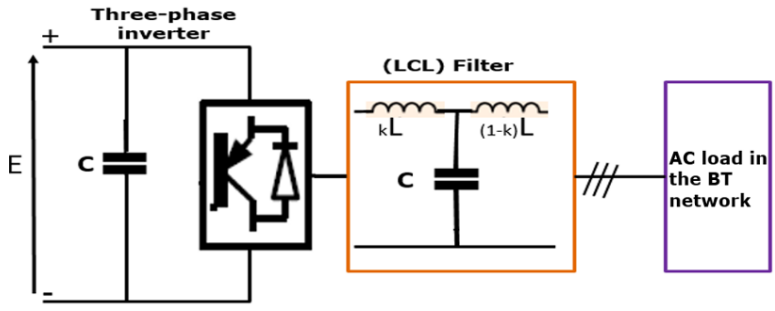

Figure 1. Supplying an AC load in the LV network.

In black is the three-phase, two-level inverter with full 180˚ control, responsible for converting the DC voltage E into a non-sinusoidal AC voltage (Figure 1).

In red is the LCL filter, responsible for attenuating and eliminating the distortion harmonics contained in the non-sinusoidal AC voltage and current signals. After the LCL filter is the rural area representing the three-phase AC load.

In our LCL filter model, inductance L is the total inductance calculated by the log method. To form the LCL filter, a coefficient varying between 0 and 1 is applied, as is done in the logs [11]. The capacitance C of the capacitor calculated in log is used in its entirety.

To the results obtained in this approach, we will associate another approach of dimensioning a damper for each L_1 and L_2 of the L_1CL_2 filter. Finally, an analysis to determine which combinations of L and C give satisfactory results.

3. Formulas for Sizing the LC Filter of the 180˚ Full Control Inverter

In the paper [12], the LC filter was used to filter the non-sinusoidal alternating signals supplied by the 180˚ fully controlled three-phase two-level inverter. The sizing was done by calculating the extreme values of the inductance of the LC filter which are:

$$L_{\text{mini}} = \frac{\sqrt{2} \times U_{ph}}{10\pi \times \sqrt{3} \times fxI_n} = \frac{0.0003 \times S_N}{I_n^2} \tag{1}$$

$$L_{\text{maxi}} = \frac{4}{(2\pi f)^2 C} \tag{2}$$

L_{mini} is the minimum value and L_{maxi} the maximum value.

In resonance,

$$\omega_{\text{Res}} = \frac{1}{\sqrt{LC}} \tag{3}$$

From Equation (3), posing $\omega = \omega_{\text{Rés}}$, we can write:

$$C_{\text{maxi}} = \frac{4}{(2\pi f)^2 L_{\text{mini}}} \tag{4}$$

For reasons of the high cost of copper noted in the paper [4], we have fixed the maximum value of the inductance based on Equation (4):

$$L_{\text{maxi}} = 4 \times L_{\text{mini}} \tag{5}$$

This allows us to write according to the resonance phenomenon:

$$C_{\text{mini}} = \frac{4}{(2\pi f)^2 L_{\text{maxi}}} \tag{6}$$

4. Determining the Expressions of the LCL Filter Elements

Consider the single-phase circuit diagram of an LCL filter given in Figure 2.

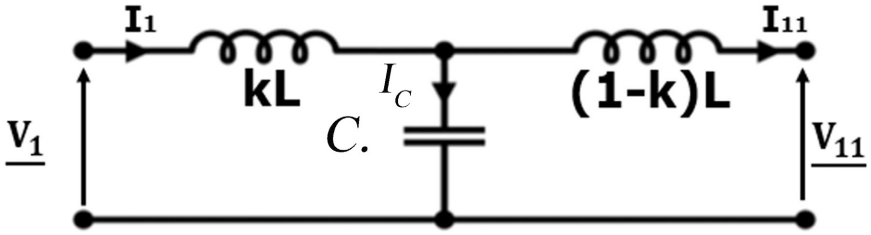

Figure 2. Single phase filter circuit (LCL).

From **Figure 2**, the transfer function H(P) can be obtained by:

$$H(P)=\frac{I_{11}(P)}{V_1(P)}=\frac{1}{LP+k(1-kL)L^2CP^3} \tag{7}$$

The resonance pulsation is :

$$\omega_{\text{Res}}=\frac{1}{\sqrt{k(1-k)LC}} \tag{8}$$

The LCL filter attenuates 60 (dB)/decade.

k is a coefficient between 0 and 1 ($0 < k < 1$).

Depending on the values of K, we present the evolution of the gain in dB and the phase in degrees as a function of the pulsation ω, illustrated in **Figure 3**.

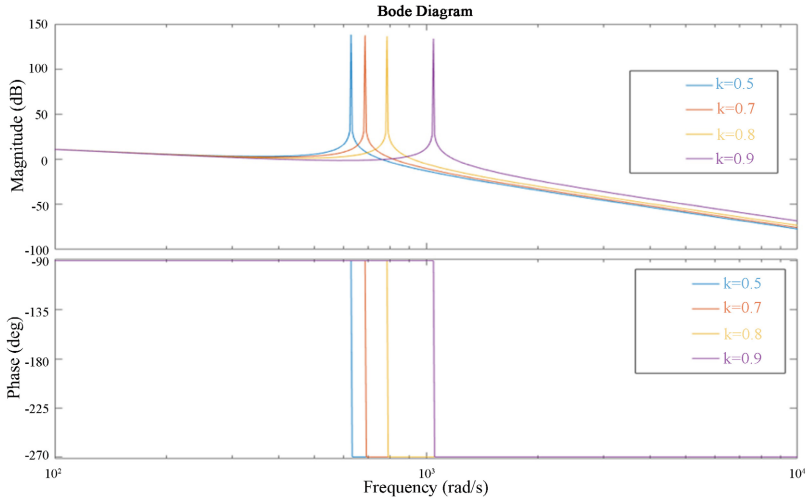

Figure 3. Bode diagram of the LCL filter according to several values of k.

Figure 3 shows that as k increases, the resonance pulsation increases; and the asymptote for $k = 0.9$ is above the asymptotes for $k < 0.9$. This means that the asymptote for $k = 0.9$ attenuates more the undesirable harmonics contained in the AC voltage and current signals. In terms of phase, there is an increase in the phase margin as k increases. This increases the degree of stability of the LCL filter.

4.1. LCL Filter Element Sizing Method

Typically, the LCL filter looks like **Figure 4**, where L_1 and L_2 are inductances

and C is the capacitance.

In our approach, we assume $L = L_1 + L_2$; L is the LC filter inductance between L_{mini} and L_{maxi}. The capacitance C is exactly that of the LC filter between C_{mini} and C_{maxi}. These optimum values were developed in [12].

In the papers [3], researchers introduced a coefficient r, such that $L_1 = r * L_2$ to give $L = (1+2) * L_2$, with $r < 1$. This coefficient r introduces a final ratio (1 + r) between L and L_2 of up to practically 2, which increases the value of inductance L. But in this paper, the coefficient *k*, such that: $0 < k < 1$, so that the value L does not exceed the sum of inductances L_1 and L_2. This is different from what was done in [13]-[15]. This allows us to write:

$L_1 = k * L$ and $L_2 = (1-k) * L$ so that: $L = L_1 + L_2$.

Here, neither L_1 nor L_2 can have a ratio reaching 1 between them and *L*. But their sum is equal to *L*. This approach reduces the iron core of L_1 and L_2.

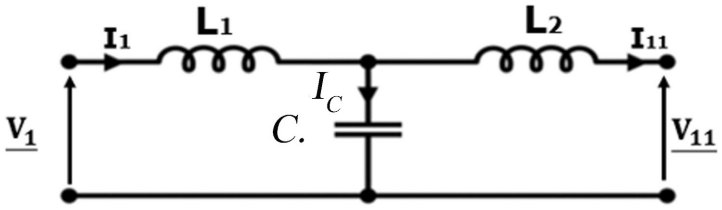

Figure 4. Single phase filter circuit (L_1CL_2).

4.2. Validation of the Method

Table 1. Simulation parameters.

PARAMETERS	VALUES
Apparent power S_N	50 kVA
Voltage between phases at the terminals of the AC load, U_{ph}	400 V
Rated current in the AC load, *In*	72.17 A
DC voltage at inverter input, E	513.02 V
Power factor cosφ	0.8
Minimum filter inductance *LC*, L_{mini}	2.88 mH
Maximum filter inductance *LC*, L_{maxi}	11.52 mH
Minimum filter capacity *LC*, C_{mini}	0.88 mF
Maximum filter capacity *LC*, C_{maxi}	3.52 mF

In the paper [12], the combinations were: (L_{mini}, C_{mini}); (L_{mini}, C_{maxi}); (L_{maxi}, C_{mini}) and (L_{maxi}, C_{maxi}). The results were obtained for the LC filter used for the three-phase two-level inverter with 180˚ full-wave control.

We apply the same combinations of the *LC* filter to the LCL filter, introducing the coefficient *k* at the inductance L between L_{mini} and L_{maxi}. We take a few values of the *k* coefficient: 0.1 to 0.9. For these values of the coefficient k, we calculate L_1 and L_2 which we present in Table 2 and Table 3.

Table 2. Values of L_1 and L_2 according to k for (L_{mini}, C_{mini}) and (L_{maxi}, C_{mini}).

k	$L = L_{mini}$		$C = C_{mini}$	$L = L_{maxi}$		$C = C_{mini}$
	L_1 (mH)	L_2 (mH)		L_1 (mH)	L_2 (mH)	
0.1	0.288	2.592	0.88 mF	1.152	10.368	0.88 mF
0.2	0.576	2.304		2.304	9.216	
0.3	0.864	2.016		3.456	8.064	
0.4	1.152	1.728		4.608	6.912	
0.5	1.44	1.44		5.76	5.76	
0.6	1.728	1.152		6.912	4.608	
0.7	2.016	0.864		8.064	3.456	
0.8	2.304	0.576		9.216	2.304	
0.9	2.592	0.288		10.368	1.152	

Table 3. Values of L_1 and L_2 according to k for (L_{mini}, C_{maxi}) and (L_{maxi}, C_{maxi}).

k	$L = L_{mini}$		$C = C_{maxi}$	$L = L_{maxi}$		$C = C_{maxi}$
	L_1 (mH)	L_2 (mH)		L_1 (mH)	L_2 (mH)	
0.1	0.288	2.592	3.52 mF	1.152	10.368	3.52 mF
0.2	0.576	2.304		2.304	9.216	
0.3	0.864	2.016		3.456	8.064	
0.4	1.152	1.728		4.608	6.912	
0.5	1.44	1.44		5.76	5.76	
0.6	1.728	1.152		6.912	4.608	
0.7	2.016	0.864		8.064	3.456	
0.8	2.304	0.576		9.216	2.304	
0.9	2.592	0.288		10.368	1.152	

4.3. Simulation of All Possible Combinations

The simulations were performed on MATLAB using an Intel ® Core™ i5; 2.50 GHz workstation. We present Figures 5-8 to illustrate the results for each combination of inductance and capacitor capacitance.

1) Case 1: Combination (L_{mini}, C_{mini})

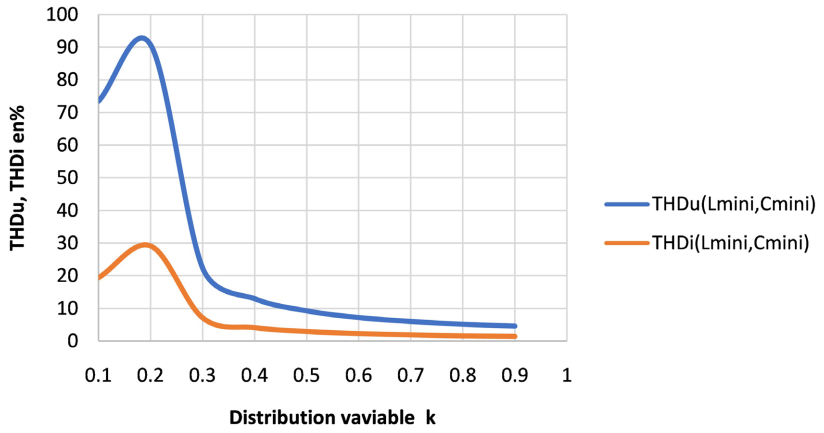

Figure 5. Evolution of THDu and THDi of the pair (L_{mini}, C_{mini}) as a function of k.

2) Case 2: Combination (L_{maxi}, C_{mini})

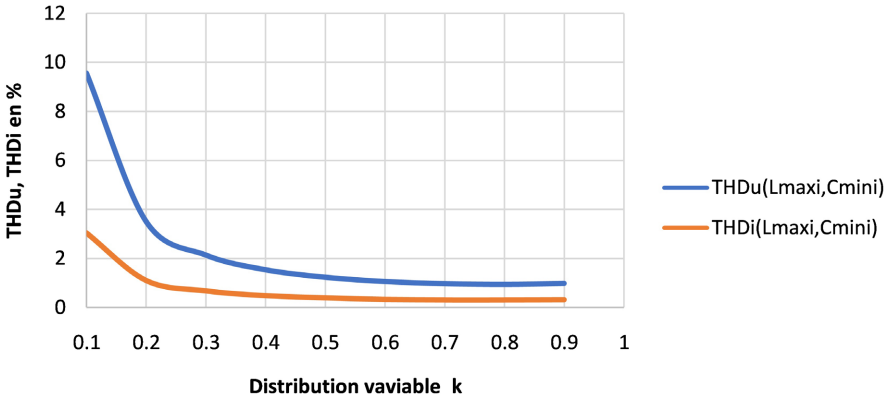

Figure 6. Evolution of THDu and THDi of the pair ($L_{maxi,}$ C_{mini}) as a function of *k*.

3) Case 3: Combination ($L_{mini,}$ C_{maxi})

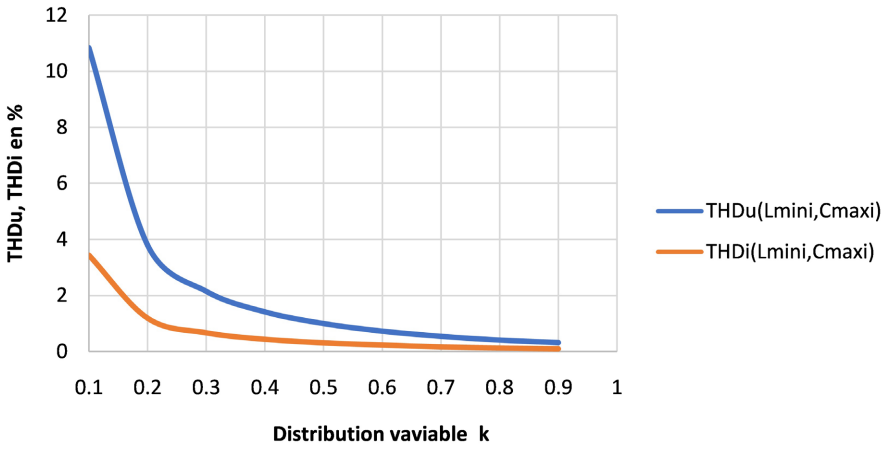

Figure 7. Evolution of THDu and THDi of the pair ($L_{mini,}$ C_{maxi}) as a function of *k*.

4) Case 4: Combination ($L_{maxi,}$ C_{maxi})

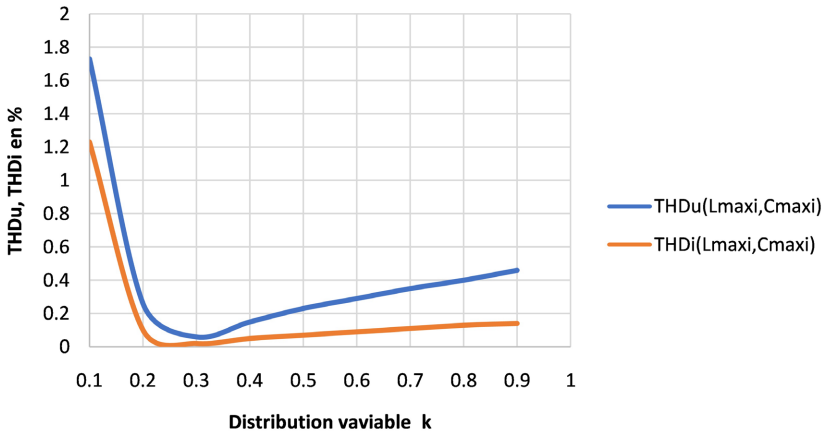

Figure 8. Evolution of THDu and THDi of the pair ($L_{maxi,}$ C_{mini}) as a function of *k*.

4.4. Analysis and Discussion

In the first case of combination (L_{mini}, C_{mini}), the voltage and current THDs comply with the IEEE 519-2014 standard only from $k = 0.6$ (see Figure 5). Before this value of k, the THDs are very high; especially the voltage THD is higher than the 8% limit value.

In the second case of combination (L_{maxi}, C_{mini}) where the value of the inductance is high, it is from $k = 0.2$ that the voltage and current THDs that comply with the IEEE 519-2014 standard. The range of k allowing compliance with the standard has increased from 0.2 to 0.9 (Figure 6).

In the third combination case (L_{mini}, C_{maxi}) where the condenser capacity value is high, the range in which the standard is met remains unchanged, *i.e.* from 0.2 to 0.9 (see Figure 7).

On the other hand, **in the fourth combination case (L_{maxi}, C_{maxi})** where we have both high inductance and capacitor capacitance values, the IEEE 519-2014 standard is met over the entire range from 0.1 to 0.9 (see Figure 8).

But the RMS current through the load is low. This means that the use of a damper to guarantee an exact value for the RMS voltage across the load is not possible, as this input will deteriorate the load and, above all, the RMS current. The same phenomenon is not observed for the combination (L_{maxi}, C_{mini}), despite the high value of the inductance.

If the economic criterion is added, only the combinations of cases 1 and 3 remain. Because the cost of copper is high on the raw materials markets.

If the criteria of size, volume and weight are added, only the combinations of cases N˚1 and N˚3 remain satisfactory. This is because the cost of copper is high on the raw materials markets. Figures 9-13 show the waveforms of the filtered voltage and current signals for the combination (L_{mini}, C_{maxi}).

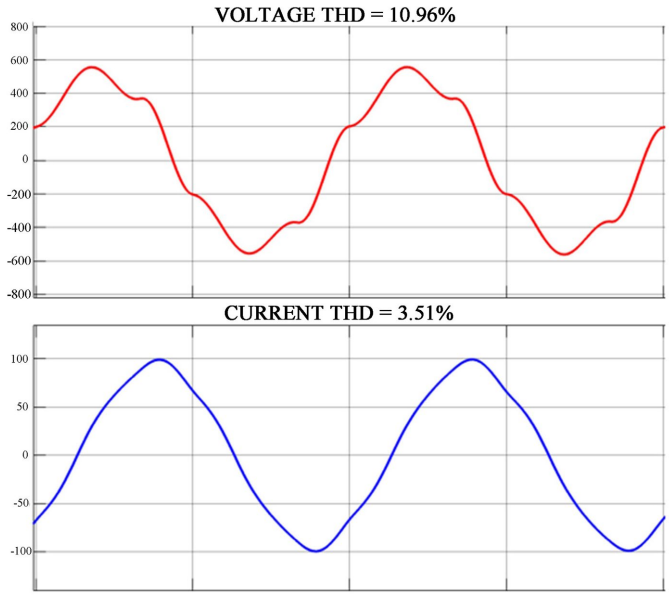

Figure 9. Voltage and current waveforms for $k = 0.1$ with $L = L_{mini}$ and $C = C_{maxi}$.

The waveforms of the filtered voltage and current signals for the combination (L_{mini}, C_{maxi}) justify compliance with the IEEE 519-2014 standard for the coefficient k belonging to the range 0.2 to 0.9. Figure 9 shows the case where the standard is not met, with THDu = 10.96% above the standard limit of 8%.

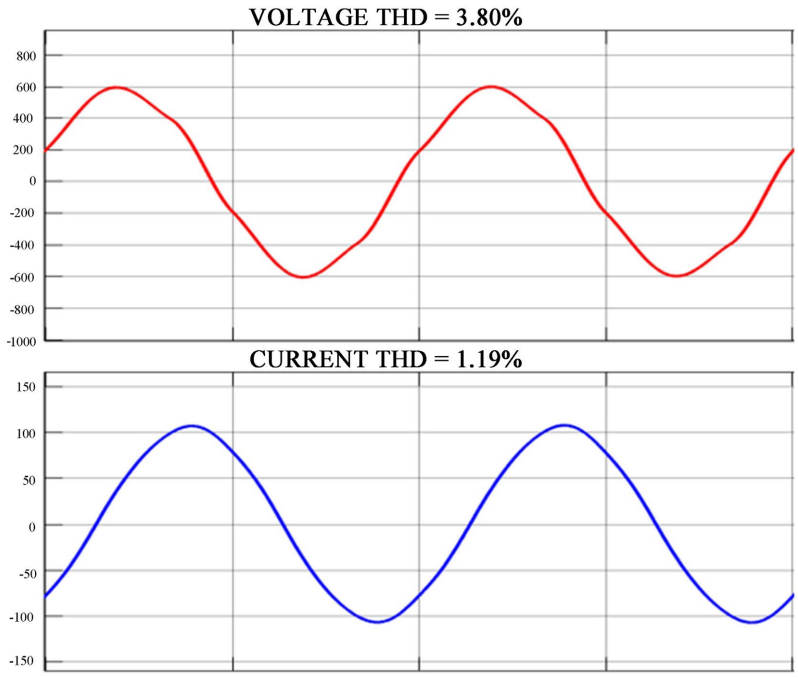

Figure 10. Voltage and current waveforms for $k = 0.2$ *with* $L = L_{mini}$ *and* $C = C_{maxi}$.

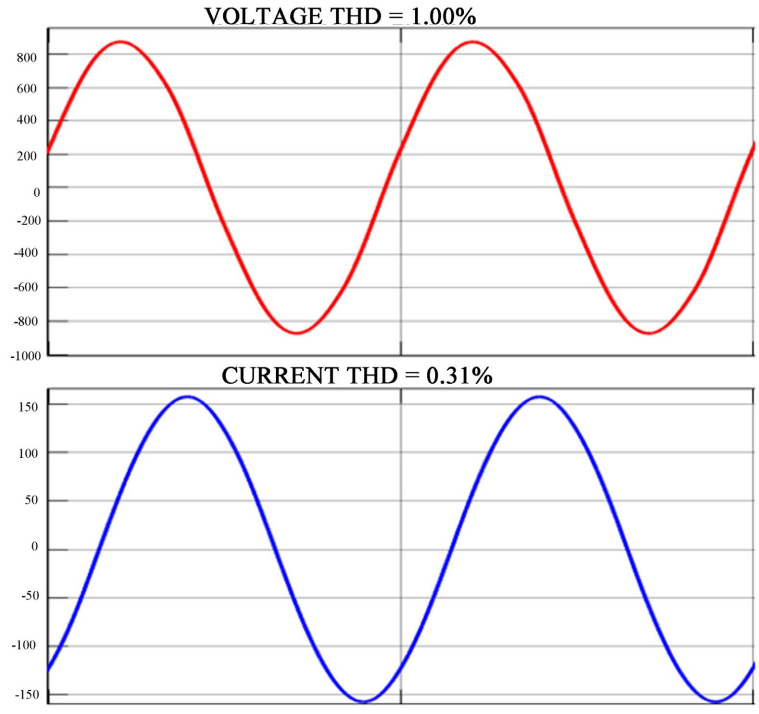

Figure 11. Voltage and current waveforms for $k = 0.5$ *with* $L = L_{mini}$ *and* $C = C_{maxi}$.

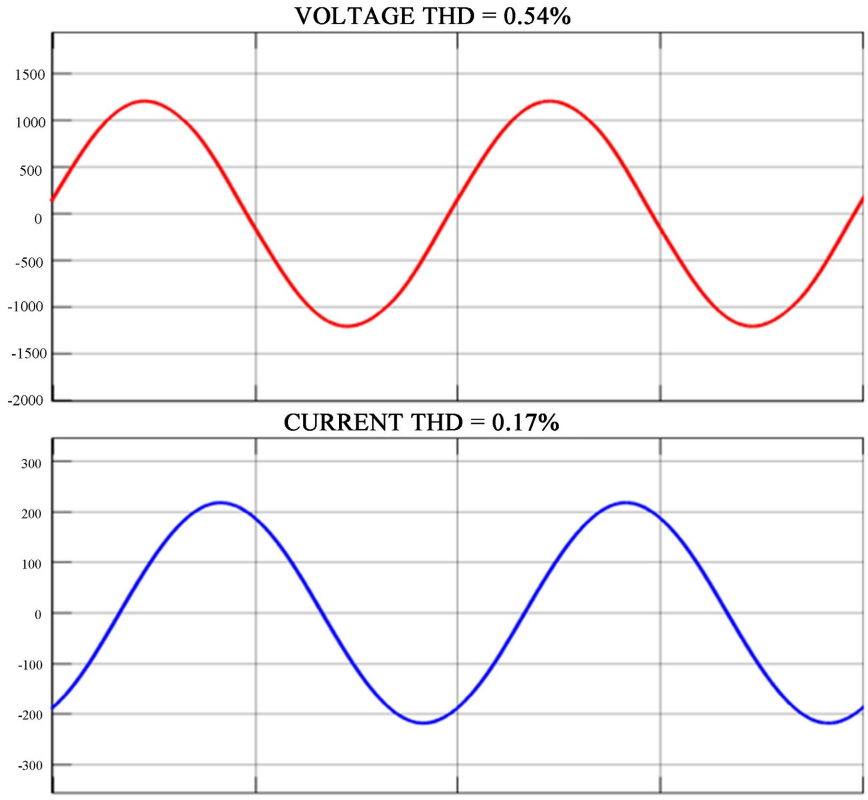

Figure 12. Voltage and current waveforms for $k = 0.7$ *with* $L = L_{mini}$ *and* $C = C_{maxi}$.

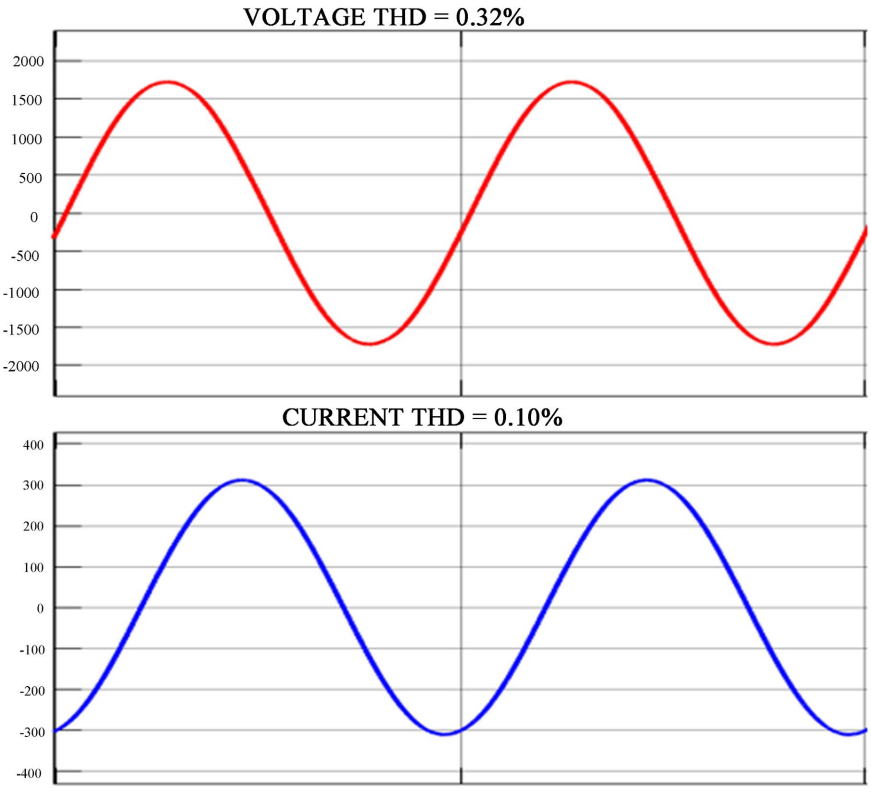

Figure 13. Voltage and current waveforms for $k = 0.9$ *with* $L = L_{mini}$ *and* $C = C_{maxi}$.

Figures 14-18 show the waveforms of the filtered voltage and current signals for the combination (L_{mini}, C_{mini}):

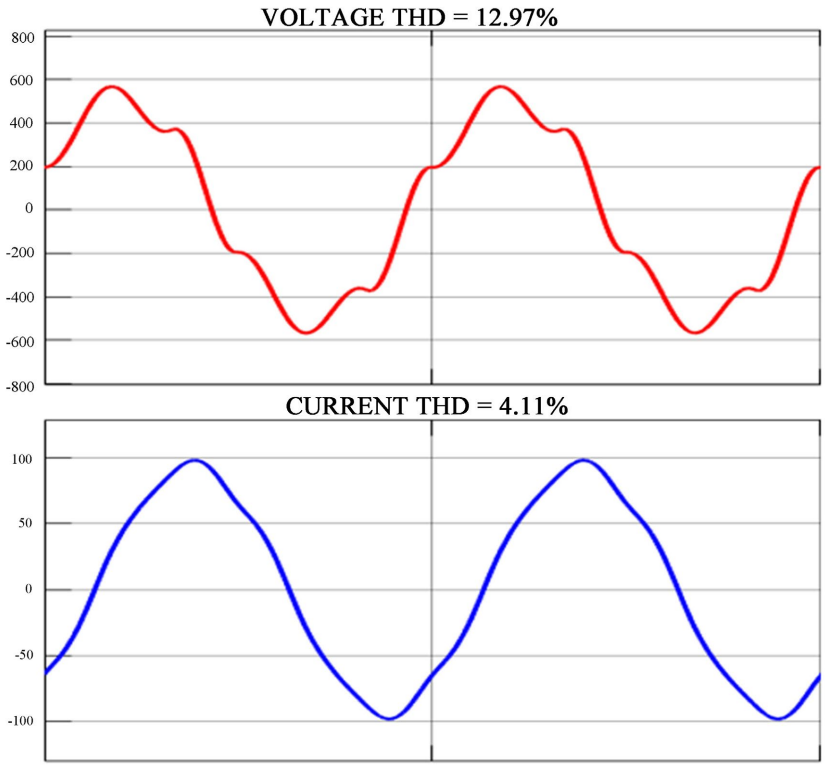

Figure 14. Voltage and current waveforms for $k = 0.4$ *with* $L = L_{mini}$ *and* $C = C_{mini}$.

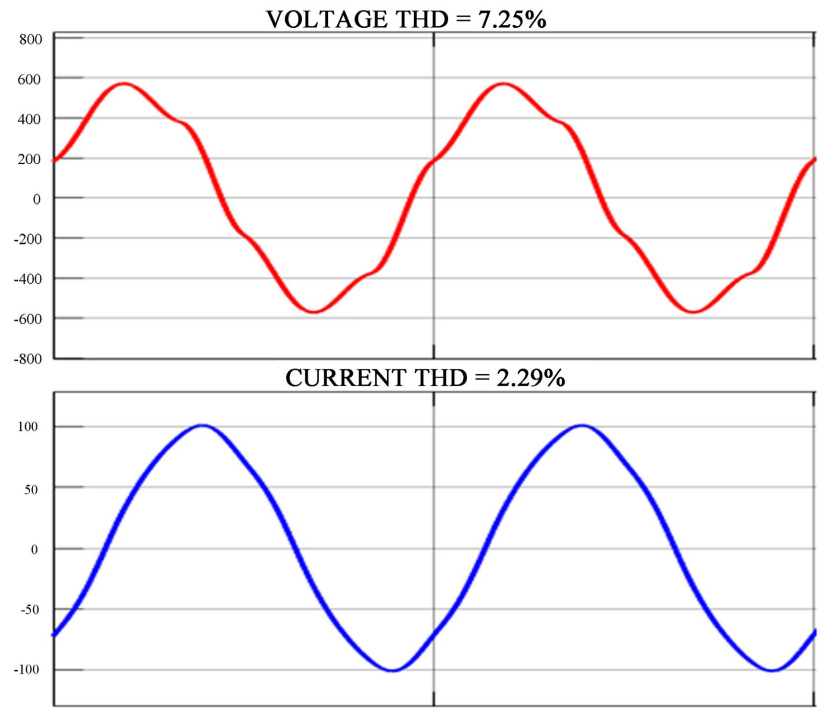

Figure 15. Voltage and current waveforms for $k = 0.6$ *with* $L = L_{mini}$ *and* $C = C_{mini}$.

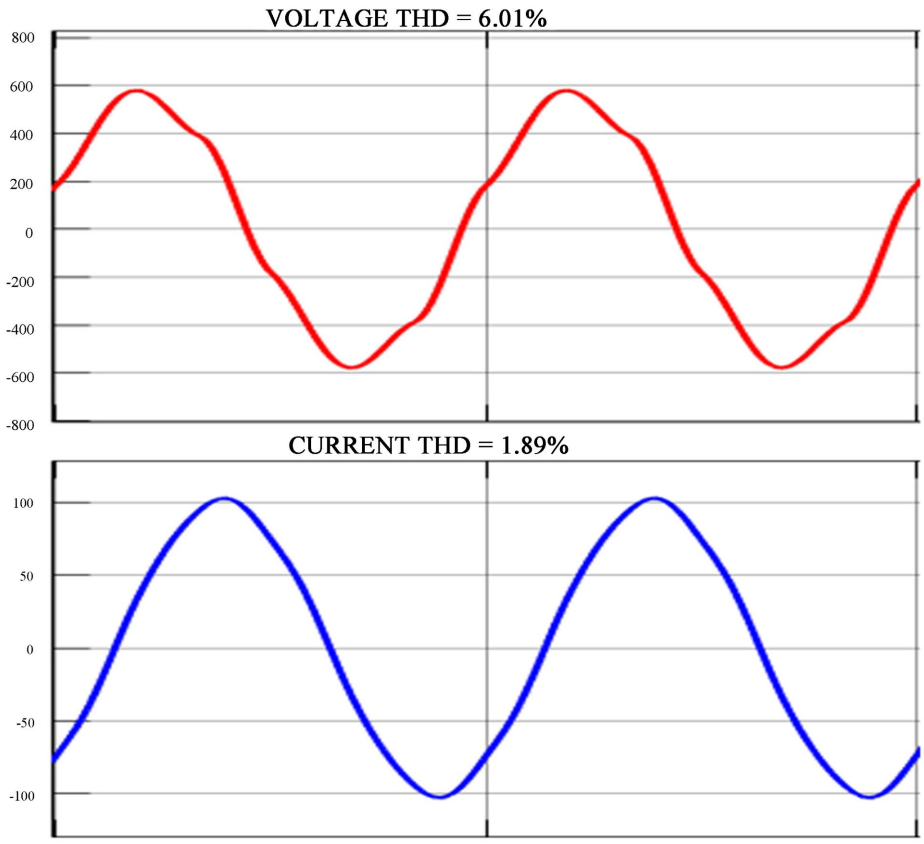

Figure 16. Voltage and current waveforms for $k = 0.7$ *with* $L = L_{mini}$ *and* $C = C_{mini}$.

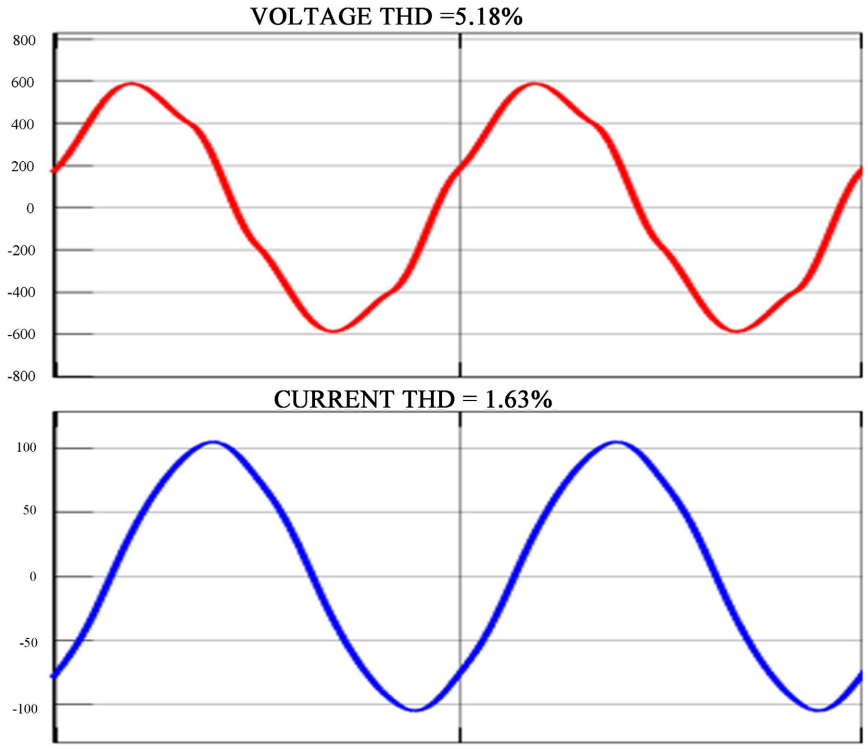

Figure 17. Voltage and current waveforms for $k = 0.8$ *with* $L = L_{mini}$ *and* $C = C_{mini}$.

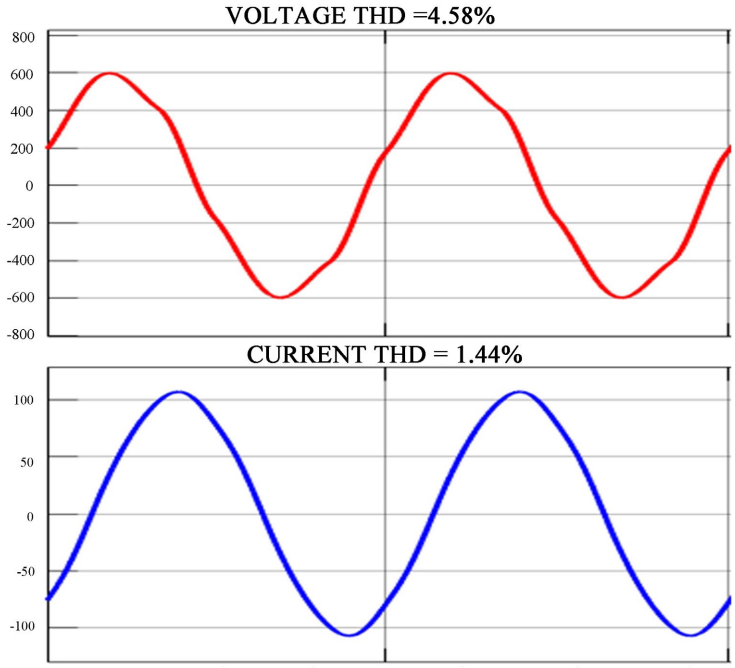

Figure 18. Voltage and current waveforms for $k = 0.9$ *with* $L = L_{mini}$ *and* $C = C_{mini}$.

The waveforms of the filtered voltage and current signals for the combination (L_{mini} ; C_{mini}) justify compliance with the IEEE 519-2014 standard for the coefficient k belonging to the range 0.6 to 0.9. **Figure 14** shows the case where the standard is not met, with THDu = 12.97% above the standard limit of 8%.

Figures 19-23 show the waveforms of the filtered voltage and current signals for the combination (L_{maxi}, C_{maxi}). The waveforms of the filtered voltage and current signals for the combination (L_{maxi}, C_{maxi}) justify compliance with the IEEE 519-2014 standard for the coefficient k varying from 0.1 to 0.9.

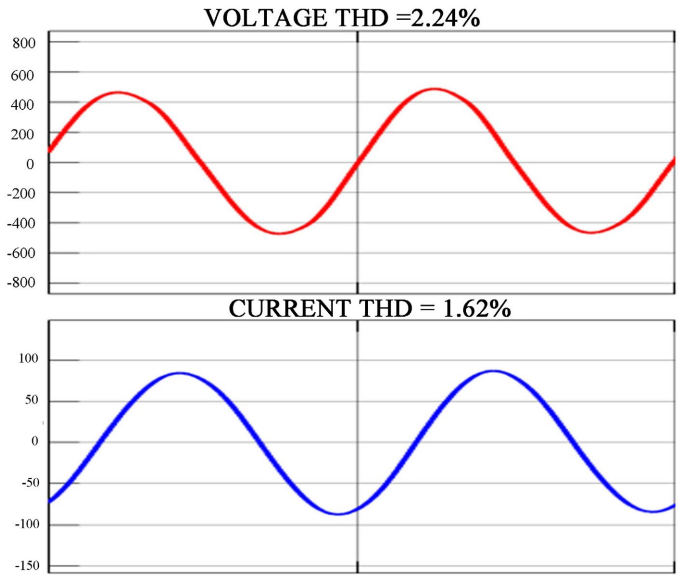

Figure 19. Voltage and current waveforms for $k = 0.1$ *with* $L = L_{maxi}$ *and* $C = C_{maxi}$.

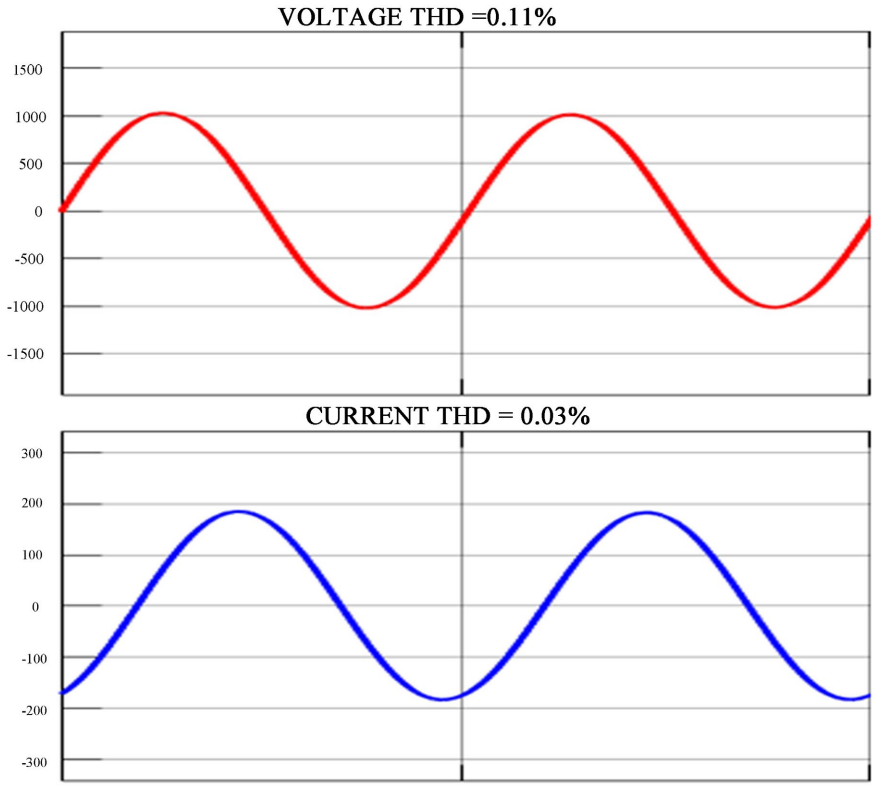

Figure 20. Voltage and current waveforms for $k = 0.2$ *with* $L = L_{maxi}$ *and* $C = C_{maxi}$.

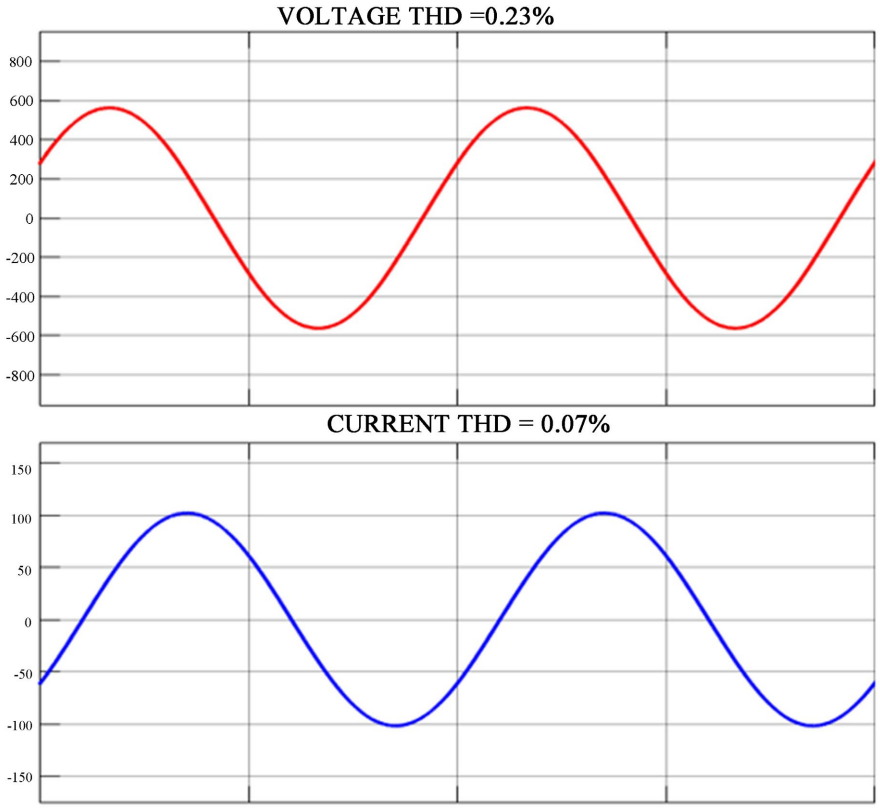

Figure 21. Voltage and current waveforms for $k = 0.5$ *with* $L = L_{maxi}$ *and* $C = C_{maxi}$.

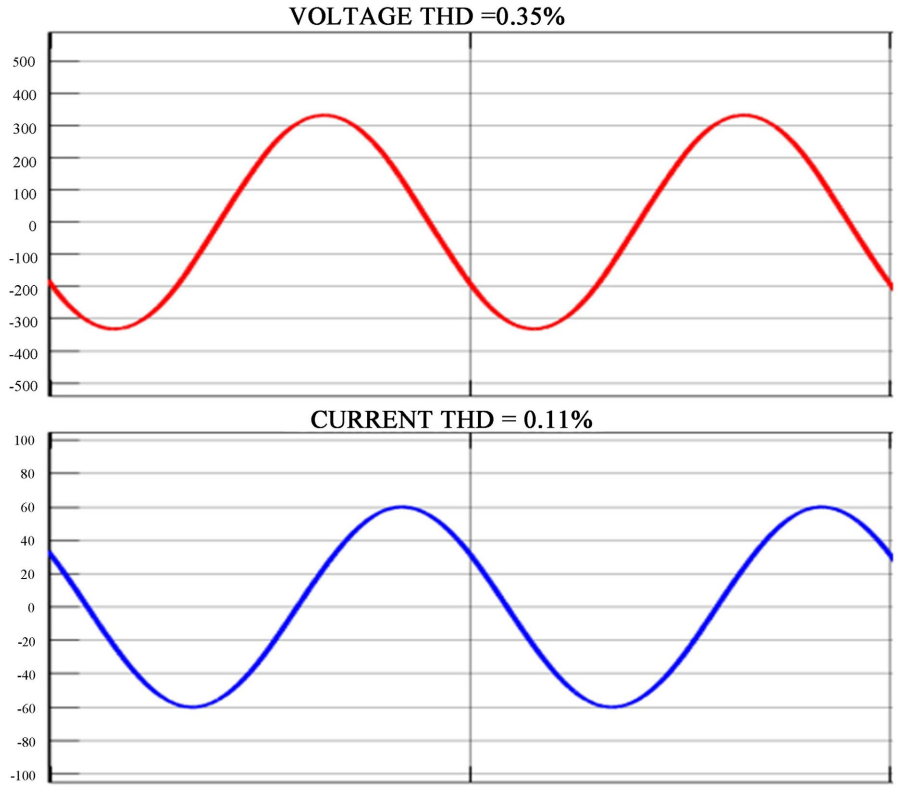

Figure 22. Voltage and current waveforms for $k = 0.7$ *with* $L = L_{maxi}$ *and* $C = C_{maxi}$.

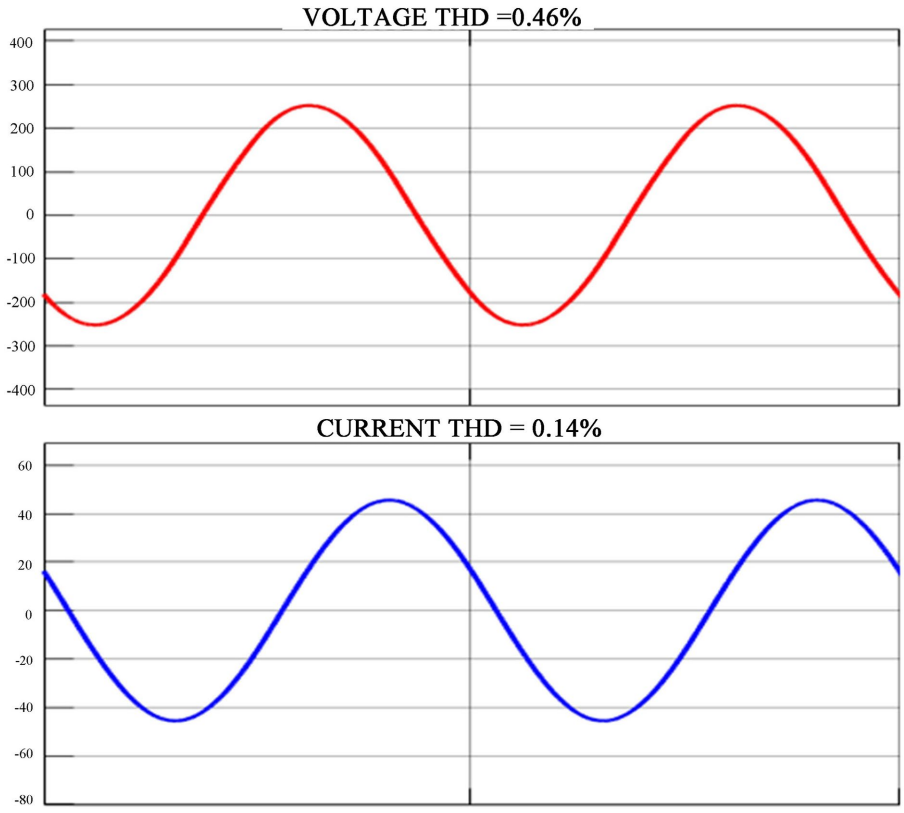

Figure 23. Voltage and current waveforms for $k = 0.9$ *with* $L = L_{maxi}$ *and* $C = C_{maxi}$.

Figures 24-28 show the waveforms of the filtered voltage and current signals for the combination (L_{maxi}, C_{mini}).

The waveforms of the filtered voltage and current signals for the combination (L_{maxi}, C_{mini}) justify compliance with the IEEE 519-2014 standard for the coefficient k belonging to the range 0.2 to 0.9. Figure 24 shows the case $k = 0.1$ where the standard is not met, with a THDu = 9.56% above the standard limit of 8%.

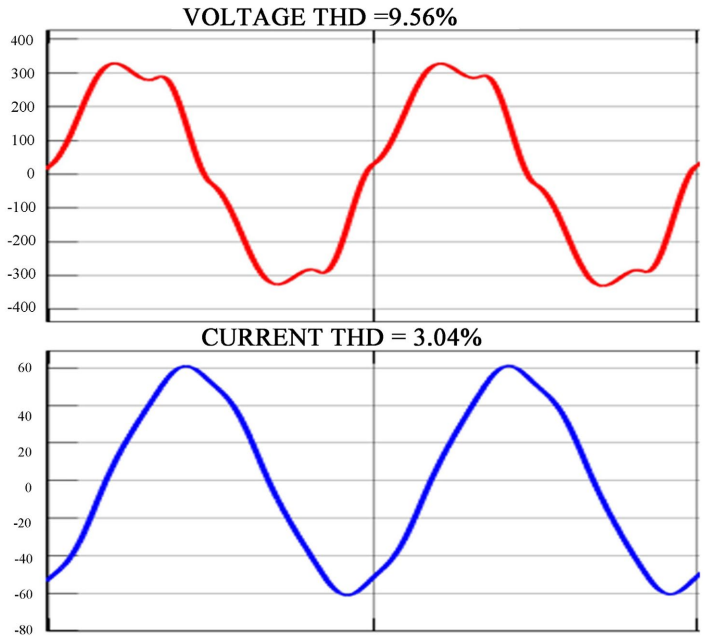

Figure 24. Voltage and current waveforms for $k = 0.1$ *with* $L = L_{maxi}$ *and* $C = C_{mini}$.

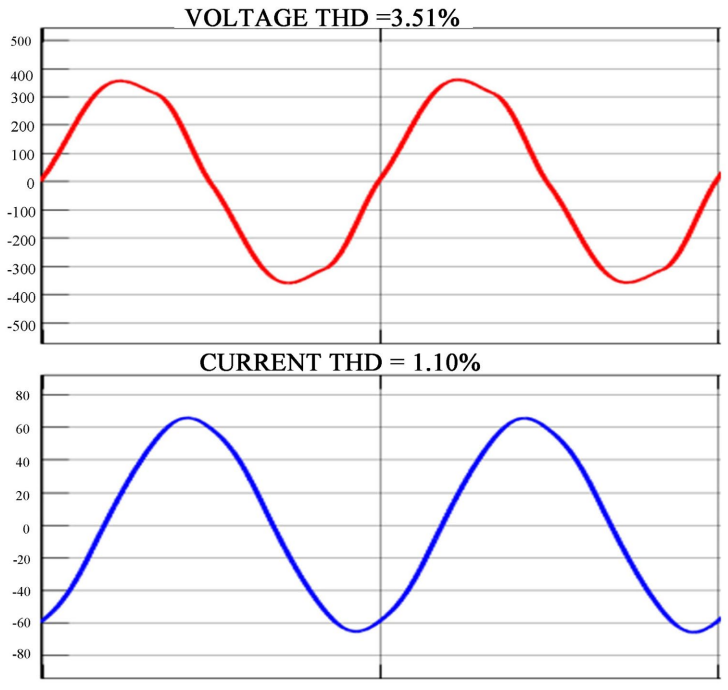

Figure 25. Voltage and current waveforms for $k = 0.2$ *with* $L = L_{maxi}$ *and* $C = C_{mini}$.

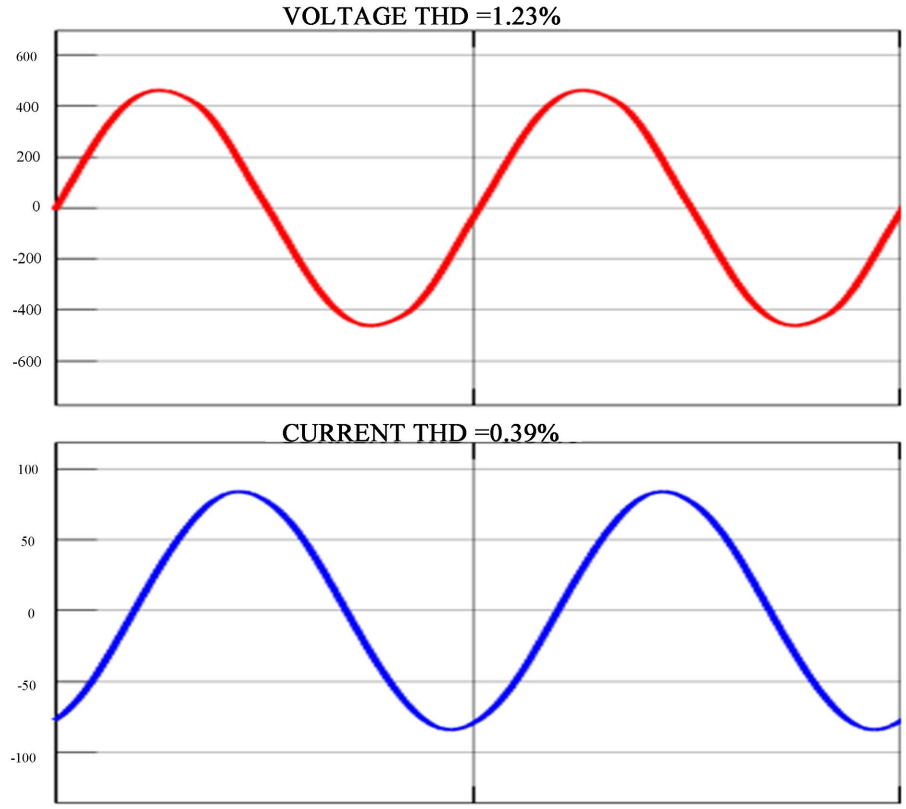

Figure 26. Voltage and current waveforms for $k = 0.5$ *with* $L = L_{maxi}$ *and* $C = C_{mini}$.

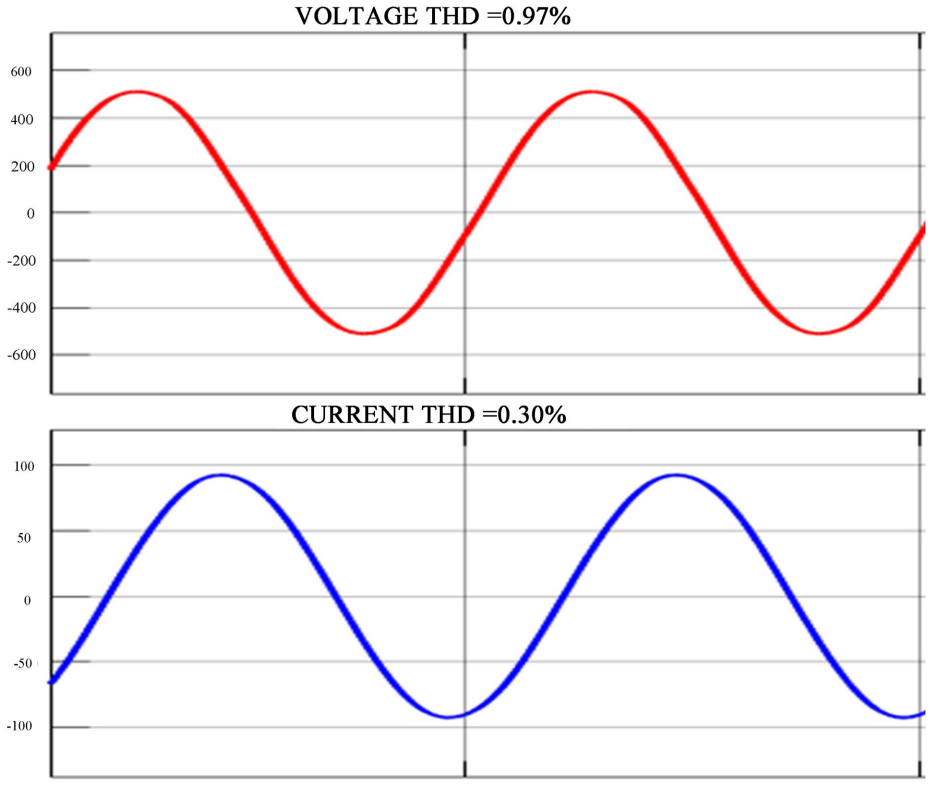

Figure 27. Voltage and current waveforms for $k = 0.7$ *with* $L = L_{maxi}$ *and* $C = C_{mini}$.

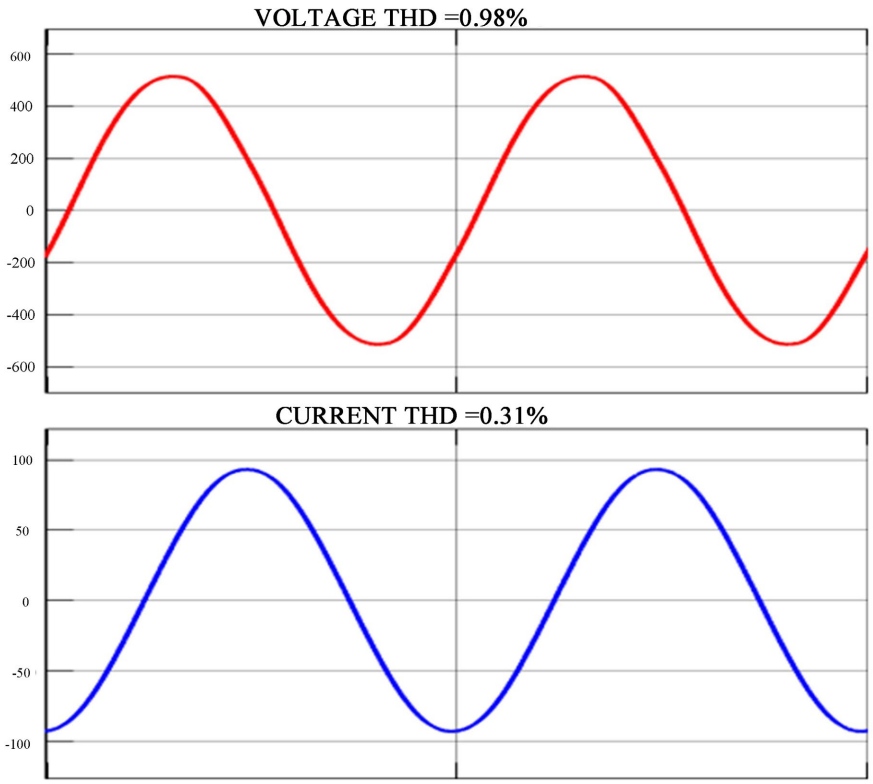

Figure 28. Voltage and current waveforms for $k = 0.9$ *with* $L = L_{maxi}$ *and* $C = C_{mini}$.

5. LCL Filter Damper Sizing Method

A filter damper is a resistor used to attenuate voltage and current amplitudes to obtain RMS voltage and current values corresponding to those required by the load. The LCL filter can have one damper for each inductor (see **Figure 29**).

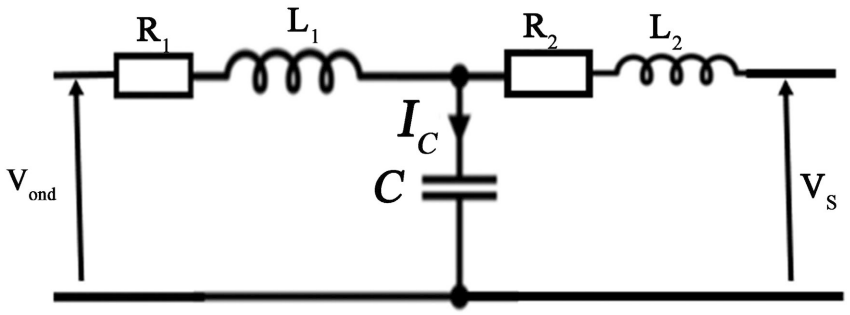

Figure 29. LCL filter with shock absorbers.

In **Figure 29**, R_1 and R_2 represent the L_1 and L_2 dampers respectively.

The approach we propose has already been developed in [16], but for the LC filter. It is based on a few properties of numerical analysis. An error rate is set at the outset. This allows convergence iterations to be carried out from a resistance consisting of:

$$R = \frac{\Delta U_{ph}}{\Delta I_n} \tag{9}$$

Where $\Delta U_{ph} = U_{phmesuree} - U_n$; $\Delta I_n = I_{nmesuree} - I_n$; U_n and I_n : rated voltage and rated load current.

Error rates are :

$$\Delta U_{ph}(\%) = \frac{U_{phmesuree} - U_n}{U_n} \times 100\% \tag{10}$$

$$\Delta I_n(\%) = \frac{I_{nmesuree} - I_n}{I_n} \times 100\% \tag{11}$$

An algorithm for performing the iterations has been developed (see Figure 30). The maximum error rate is set at 0.2%.

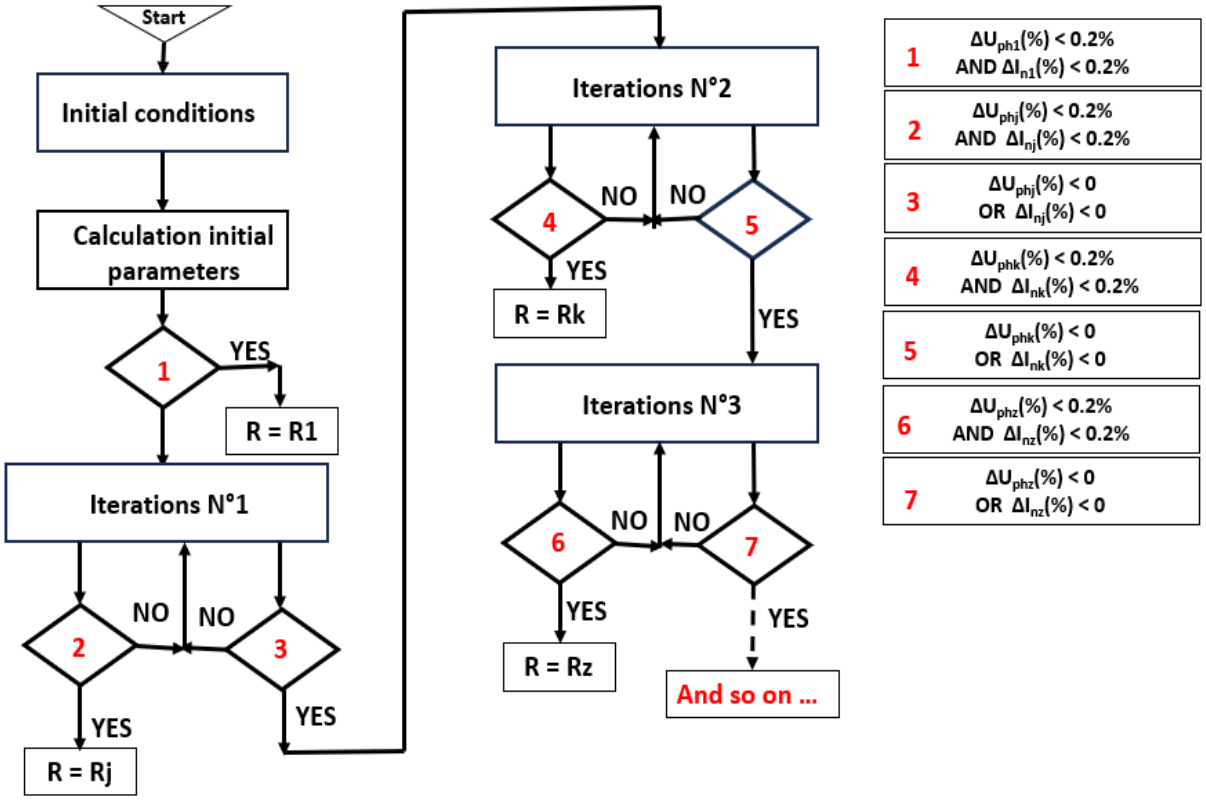

Figure 30. Flowchart of the algorithm for determining damper values.

This algorithm is used to size the resistance of each inductor in the LCL filter.

The inductance and capacitor capacitance values are given by the simulation parameters defined by the section (Table 1).

5.1. For the Combination (L_{mini}, C_{mini})

We found that from $k = 0.1$ to 0.7, it's impossible to use a damper, because for $R_1 = 0$ and $R_2 = 0$, the RMS values of voltage and current are lower than the nominal

RMS values (see Table 4). The iterations are long, so those shown in the tables are just a few lines.

Table 4. Sizing results for dampers R_1 and R_2 for $k = 0.7$ (LCL Filter).

		L_{mini} = 2.88 mH		$C = C_{mini}$	$k = 0.7$					
R1 (Ω)	R2 (Ω)	L_1 (mH)	L_2 (mH)	C (mF)	U_{ph} (V)	I_n (A)	ΔU_{ph} (%)	ΔI_n (%)	THDi (%)	THDu (%)
0	0	2.016	0.864	0.88	396.5	71.54	−0.875	−0.87	1.89	6.01
1	1	2.016	0.864	0.88	267.9	48.33	−33.025	−33	2.52	8.02
0.5	0.5	2.016	0.864	0.88	324	58.45	−19	−19	2.24	7.12
0.3	0.3	2.016	0.864	0.88	350.8	63.29	−12.3	−12.3	2.11	6.7
0.2	0.2	2.016	0.864	0.88	365.3	65.9	−8.675	−8.69	2.04	6.47
0.1	0.1	2.016	0.864	0.88	380.5	68.65	−4.875	−4.88	1.97	6.25

Table 4 shows that ΔU_{ph} (%) < 0 and ΔI_n (%) < 0, so there's no way of obtaining values for R_1 and R_2 so that ΔU_{ph} (%) and ΔI_n (%) are below the error rate set at a maximum of 0.2%.

However, for $k = 0.8$ and 0.9, we were able to dimension R_1 and R_2 (see Tables 5-6).

Table 5. Sizing results for dampers R_1 and R_2 for $k = 0.8$ (LCL Filter).

		L_{mini} = 2.88 mH		$C = C_{mini}$	$k = 0.8$					
R_1 (Ω)	R_2 (Ω)	L_1 (mH)	L_2 (mH)	C (mF)	U_{ph} (V)	I_n (A)	ΔU_{ph} (%)	ΔI_n (%)	THDi (%)	THDu (%)
0	0	2.016	0.864	0.88	405.2	73.11	1.3	1.3	1.63	5.18
1	1	2.016	0.864	0.88	271.9	49.06	−32.025	−32.02	2.22	7.09
0.05	0.05	2.016	0.864	0.88	396.8	71.59	−0.8	−0.8	1.66	5.28
0.02	0.02	2.016	0.864	0.88	401.8	72.5	0.45	0.46	1.64	5.22
0.021	0.021	2.016	0.864	0.88	401.7	72.47	0.425	0.42	1.64	5.22
0.022	0.022	2.016	0.864	0.88	401.5	72.44	0.375	0.37	1.64	5.22
0.023	0.023	2.016	0.864	0.88	401.3	72.41	0.325	0.33	1.64	5.23
0.024	0.024	2.016	0.864	0.88	401.2	72.38	0.3	0.29	1.64	5.23
0.025	0.025	2.016	0.864	0.88	401	72.35	0.25	0.25	1.64	5.23
0.026	0.026	2.016	0.864	0.88	400.8	72.31	0.2	0.19	1.65	5.23

The last of Table 5 shows that for $R_1 = R_2 = 0.026\Omega$, ΔU_{ph} (%) < 0.2% and ΔI_n (%) < 0.19%. The red lines show that ΔU_{ph} (%) and ΔI_n (%) are negative. In black, these are some iterations showing ΔU_{ph} (%) and ΔI_n (%) positive but not less than or equal to 0.2%.

Table 6. Sizing results for dampers R_1 and R_2 for $k = 0.9$ (Filter LCL).

		L_{mini} = 2.88 mH		$C = C_{mini}$	$k = 0.9$					
R_1 (Ω)	R_2 (Ω)	L_1 (mH)	L_2 (mH)	C (mF)	U_{ph} (V)	I_n (A)	ΔU_{ph} (%)	ΔI_n (%)	THDi (%)	THDu (%)
0	0	2.016	0.864	0.88	413.9	74.67	3.475	3.46	1.44	4.58
1	1	2.016	0.864	0.88	275.9	49.77	−31.025	−31.04	2	6.39
0.1	0.1	2.016	0.864	0.88	396.6	71.55	−0.85	−0.86	1.5	4.77
0.09	0.09	2.016	0.864	0.88	398.3	71.85	−0.425	−0.44	1.49	4.75
0.08	0.08	2.016	0.864	0.88	400	72.16	0	−0.01	1.49	4.73
0.07	0.07	2.016	0.864	0.88	401.7	72.47	0.425	0.42	1.48	4.17
0.077	0.077	2.016	0.864	0.88	400.5	72.25	0.125	0.11	1.48	4.72

The last of Table 6 shows that for $R_1 = R_2 = 0.077\Omega$, $\Delta U_{ph}(\%) < 0.125\%$ and $\Delta I_n(\%) < 0.11\%$. The red lines show that $\Delta U_{ph}(\%)$ and $\Delta I_n(\%)$ are negative. In black, these are some iterations showing $\Delta U_{ph}(\%)$ and $\Delta I_n(\%)$ positive but not less than or equal to 0.2%.

5.2. For the Combination (L_{mini}, C_{maxi})

For this combination, dampers R_1 and R_2 can be sized, because for $R_1 = R_2 = 0$ and for $k = 0.1$ to 0.9, the RMS values of voltage and current are higher than the nominal RMS values Un and In. Table 7 shows the results for $k = 0.7$.

The last of Table 7 shows that for $R_1 = R_2 = 0.552\Omega$, $\Delta U_{ph}(\%) < 0.125\%$ and $\Delta I_n(\%) < 0.12\%$. The red lines show that $\Delta U_{ph}(\%)$ and $\Delta I_n(\%)$ are negative. In black, these are some iterations showing $\Delta U_{ph}(\%)$ and $\Delta I_n(\%)$ positive but not less than or equal to 0.2%.

Table 7. Sizing results for dampers R_1 and R_2 for $k = 0.7$.

		L_{mini} = 2.88 mH		$C = C_{mini}$	$k = 0.7$					
R_1 (Ω)	R_2 (Ω)	L_1 (mH)	L_2 (mH)	C (mF)	U_{ph} (V)	I_n (A)	ΔU_{ph} (%)	ΔI_n (%)	THDi (%)	THDu (%)
0	0	2.016	0.864	3.52	852	153.7	113	112.97	0.17	0.54
1	1	2.016	0.864	3.52	244.2	44.05	−38.95	−38.96	0.55	1.76
0.55	0.55	2.016	0.864	3.52	401.5	72.44	0.375	0.37	0.35	1.12
0.56	0.56	2.016	0.864	3.52	396.5	71.54	−0.875	−0.87	0.35	1.14
0.551	0.551	2.016	0.864	3.52	401	72.35	0.25	0.25	0.35	1.14
0.552	0.552	2.016	0.864	3.52	400.5	72.26	0.125	0.12	0.35	1.12

5.3. For the Combination (L_{maxi}, C_{mini})

For this combination, there is no possibility of sizing dampers R_1 and R_2, because for $R_1 = R_2 = 0$ and for $k = 0.1$ to 0.9; the RMS values of voltage and current are lower than the nominal RMS values Un and In. Table 8 shows the results for $k = 0.7$.

Table 8. Sizing results for dampers R_1 and R_2 for $k = 0.7$.

		L_{mini} = 2.88 mH		$C = C_{mini}$	$k = 0.7$					
R_1 (Ω)	R_2 (Ω)	L_1 (mH)	L_2 (mH)	C (mF)	U_{ph} (V)	I_n (A)	ΔU_{ph} (%)	ΔI_n (%)	THDi (%)	THDu (%)
0	0	8.064	3.456	0.88	363.8	65.62	−9.05	−9.08	0.3	0.97
1	1	8.064	3.456	0.88	279	50.33	−30.25	−30.26	0.39	1.24
0.5	0.5	8.064	3.456	0.88	321.2	57.95	−19.7	−19.7	0.34	1.09
0.3	0.3	8.064	3.456	0.88	338.4	61.06	−15.4	−15.39	0.32	1.04
0.2	0.2	8.064	3.456	0.88	347	62.6	−13.25	−13.26	0.32	1.01
0.1	0.1	8.064	3.456	0.88	355.5	64.13	−11.125	−11.14	0.31	0.99

We found that for $k = 0.1$ to 0.9 and $R_1 = R_2 = 0$, the measured rms values of voltage and current are all below the nominal rms values U_n and I_n.

Table 8 shows that ΔU_{ph} (%) < 0 and ΔI_n (%) < 0, so there is no possibility of obtaining values of R1 and R2 so that ΔU_{ph} (%) and ΔI_n (%) are less than or equal to the error rate set at a maximum of 0.2%.

5.4. For the Combination (L_{maxi}, C_{maxi})

For this combination, there is no possibility of sizing dampers R_1 and R_2, because for $R_1 = R_2 = 0$ and for $k = 0.1$ to 0.9; the RMS values of voltage and current are lower than the nominal RMS values Un and In. Table 9 shows the results for $k = 0.7$.

We noticed that for $k = 0.1$ to 0.9 and $R_1 = R_2 = 0$, the measured RMS voltage and current values are all lower than the nominal RMS values U_n and I_n.

Table 9 shows that ΔU_{ph} (%) < 0 and ΔI_n (%) < 0, so there is no possibility of obtaining values of R_1 and R_2 so that ΔU_{ph} (%) and ΔI_n (%) are less than or equal to the error rate set at a maximum of 0.2%.

Table 9. Sizing results for dampers R_1 and R_2 for $k = 0.7$.

		L_{mini} = 2.88 mH		$C = C_{mini}$	$k = 0.7$					
R_1 (Ω)	R_2 (Ω)	L_1 (mH)	L_2 (mH)	C (mF)	U_{ph} (V)	I_n (A)	ΔU_{ph} (%)	ΔI_n (%)	THDi (%)	THDu (%)
0	0	8.064	3.456	3.52	235.4	42.47	−41.15	−41.15	0.11	0/35
1	1	8.064	3.456	3.52	145.4	26.23	−63.65	−63.66	0.17	0.55
0.5	0.5	8.064	3.456	3.52	188.8	34.06	−52.8	−52.81	0.13	0.43
0.3	0.3	8.064	3.456	3.52	207.8	37.48	−48.05	−48.07	0.12	0.39
0.2	0.2	8.064	3.456	3.52	217.2	39.19	−45.7	−45.7	0.12	0.37
0.1	0.1	8.064	3.456	3.52	226.5	40.86	−43.375	−43.38	0.12	0.36

6. Analysis of Results

The aim of this work is to use the parameters of the LC filter of the 180˚-controlled three-phase two-level inverter to construct an LCL filter for the same inverter by

introducing a coefficient k varying between 0.1 and 0.9 on the one hand; and on the other hand to dimension the dampers of the different LCL filters and deduce the classification of the combinations by taking into account the cost, weight, volume and damping of the filtered load signals.

The results show that for all combinations and for k ranging from 0.1 to 0.9, the voltage and current THDs comply with the IEEE 519-2014 standard. Except for (L_{mini}, C_{mini}), for which compliance with IEEE 519-2014 is only possible for k ranging from 0.6 to 0.9.

An approach based on numerical analysis has been applied to all LCL filter combinations to size the various dampers. The results are satisfactory for the combination (L_{mini}, C_{maxi}) for k ranging from 0.1 to 0.9, as it is possible to size for this combination. It is also possible to do so for k = 0.8 and 0.9 for the (L_{mini}, C_{mini}) combination. There is no possibility for the other combinations, as in the remaining cases the inductances are high. They therefore cause a high voltage drop. This makes it impossible to use dampers to stabilize RMS voltage and current values.

If, in addition to damping, we consider cost, weight, volume and overall dimensions, we can easily say that the best combination is (L_{mini}, C_{maxi}) for k ranging from 0.1 to 0.9. The combination (L_{mini}, C_{mini}) is also interesting for only k = 0.8 and 0.9.

Generally, we can say that combinations where the inductance value is minimal cause less voltage drop. The L_1 and L_2 coils don't require a large iron core because of the low value of Lmini. The number of turns should therefore be lower, depending on the dampers R_1 and R_2.

Comparison of the performance of LC and LCL filters in compliance with the IEEE 519-2014 standard.

Looking at Table 10, we can see that the LCL filter has lower-value dampers than the LC filter. This could result in fewer joule losses for the same current. But its voltage and current THD values are higher than those of the LC filter.

Table 10. LC vs LCL filter comparison.

LC Filter				LCL Filter				
Combinations	THDu (%)	THDi (%)	Damper R (Ω)	k	THDu (%)	THDi (%)	Dampers (Ω)	
							R_1	R_2
(L_{mini}, C_{mini})	4.37	1.37	0.2	0.9	4.58	1.44	0.077	0.077
(L_{mini}, C_{maxi})	0.89	0.28	0.767	0.9	0.94	0.29	0.6125	0.6125
(L_{maxi}, C_{mini})	1.08	0.34		0.75	0.95	0.3		
				0.25	0.11	0.03		
(L_{maxi}, C_{maxi})	0.55	0.17	Impossible	0.5	0.23	0.07	Impossible	
				0.75	0.37	0.12		
				0.9	0.46	0.14		

For the combination (L_{mini}, C_{maxi}), voltage and current THDs are significantly

the same. The LCL filter could lose more Joule losses than the LC filter, due to the virtually equal damper values. Here, filter volume, weight and size could make the difference.

The (L_{maxi}, C_{mini}) and (L_{maxi}, C_{maxi}) combinations are not recommended because of their high voltage drop.

7. Conclusions

Our method was to construct an LCL filter from the results of the LC filter dimensioned in the paper [12] and a coefficient k varying between 0 and 1, so that the sum of the inductances L1 and L2 of the LCL filter is equal to the inductance L of the LC filter. The inductance L is positioned between L_{mini} and L_{maxi} on the one hand; and on the other hand, dimension their dampers using a numerical analysis approach.

All combinations (L_{mini}, C_{mini}); (L_{mini}, C_{maxi}); (L_{maxi}, C_{mini}) and (L_{maxi}, C_{maxi}) were tested on the 180˚-controlled three-phase two-level inverter on MATLAB R2016a software. The results of each combination make it possible to set the coefficient k range where the voltage and current THDs comply with the IEEE 519-2014 standard. The dampers could, therefore, only be sized for the combinations (L_{mini}, C_{mini}) for $k = 0.8$ and 0.9; and (L_{mini}, C_{maxi}) for $k = 0.1$ to 0.9.

If we consider the high cost of copper on the raw materials markets, volume, weight and bulk, a classification of combinations is possible for the LCL filter according to k ranges.

The combination (L_{mini}, C_{mini}) would be the most advisable for $k = 0.8$ and 0.9. It is followed by (L_{mini}, C_{maxi}) for k between 0.1 and 0.9; and secondly for the possibility of using a damper to correctly set the RMS values of load voltage and current.

Conflicts of Interest

The authors declare no conflicts of interest regarding the publication of this paper.

References

[1] IEEE (2014) IEEE 519-2014, IEEE Recommended Practice and Requirements for Harmonic Control in Electric Power Systems.

[2] Sufyan, A., Jamil, M., Ghafoor, S., Awais, Q., Ahmad, H.A., Khan, A.A., *et al.* (2022) A Robust Nonlinear Sliding Mode Controller for a Three-Phase Grid-Connected Inverter with an LCL Filter. *Energies*, **15**, Article 9428. https://doi.org/10.3390/en15249428

[3] Gonçalves, D., Farias, J.V.M., Pereira, H.A., Luiz, A.A., Stopa, M.M. and Cupertino, A.F. (2022) Design of Damping Strategies for LC Filter Applied in Medium Voltage Variable Speed Drive. *Energies*, **15**, Article 5644. https://doi.org/10.3390/en15155644

[4] Bolsi, P.C., Prado, E.O., Sartori, H.C., Lenz, J.M. and Pinheiro, J.R. (2022) LCL Filter Parameter and Hardware Design Methodology for Minimum Volume Considering Capacitor Lifetimes. *Energies*, **15**, Article 4420. https://doi.org/10.3390/en15124420

[5] Li, Z., Yang, L., Yang, D., Peng, Z., Shao, D. and Liu, J. (2022) Indirect Current Con-

trol Method Based on Reference Current Compensation of an LCL-Type Grid-Connected Inverter. *Energies*, **15**, Article 965. https://doi.org/10.3390/en15030965

[6] Hussain, M.W. and Ayaz Qureshi, M. (2021) Analysis and Design of Passive Filters for Power Quality Improvement in 3ϕ Grid-Tied PV Systems. 2021 4*th International Conference on Energy Conservation and Efficiency* (*ICECE*), Lahore, 16-17 March 2021, 1-6. https://doi.org/10.1109/icece51984.2021.9406278

[7] Chakroun, R., Ayed, R.B. and Derbel, N. (2020) Comparison between LCL and LLCL Filters for a Grid Connected Inverter Using Selective Harmonic Modulation. 2020 5*th International Conference on Renewable Energies for Developing Countries* (*REDEC*), Marrakech, 29-30 June 2020, 1-6. https://doi.org/10.1109/redec49234.2020.9163595

[8] Hameed, Z., Yousaf, A., Khan, W.A., Sial, M.R.K., Ahmad, F. and Ghafoor, Z. (2020) Designing of LLCL Filter for Mitigation of Harmonics in Smart Grid Applications and Its Implementation on Sapphire Textile Industry Unit-3. 2020 *International Conference on Emerging Trends in Smart Technologies* (*ICETST*), Karachi, 26-27 March 2020, 1-6. https://doi.org/10.1109/icetst49965.2020.9080744

[9] Cai, P., Wu, X., Yang, Y., Yao, W. and Blaabjerg, F. (2020) Analysis and Design of Robust LLCL-Type Filters for Grid-Tied Applications with Capacitor-Current Active Damping. 2020 *IEEE* 9*th International Power Electronics and Motion Control Conference* (*IPEMC* 2020-*ECCE Asia*), Nanjing, 29 November-2 December 2020, 785-791. https://doi.org/10.1109/ipemc-ecceasia48364.2020.9367919

[10] Park, K. and Burkart, R.M. (2018) Filter Hardware Optimization of Grid-Tied Converters: LCL vs. LLCL Filter. 2018 7*th International Conference on Renewable Energy Research and Applications* (*ICRERA*), Paris, 14-17 October 2018, 209-214. https://doi.org/10.1109/icrera.2018.8566781

[11] Wu, Z.D. (2018) A Novel Design Method of LCL Filters for Optimal Reactive Power Compensation in Microgrids. 2018 *IEEE International Power Electronics and Application Conference and Exposition*, Shenzhen, 4-7 November 2018, 1-5.

[12] Koffi, K.F., Konaté, A., Bamba, A., Asseu, O. and Loum, G. (2021) Calculation of the Parameters of a Filter (L-C) for a 180° Control Inverter Operating in HTA. *International Journal of Materials Engineering and Technology*, **20**, 57-71. https://doi.org/10.17654/mt020010057

[13] Zeng, G., Rasmussen, T.W. and Teodorescu, R. (2010) A Novel Optimized LCL-Filter Designing Method for Grid Connected Converter. *The* 2*nd International Symposium on Power Electronics for Distributed Generation Systems*, Hefei, 16-18 June 2010, 802-805. https://doi.org/10.1109/pedg.2010.5545882

[14] Popescu, M., Bitoleanu, A. and Suru, V. (2016) On the Design of LCL Filter with Passive Damping in Three-Phase Shunt Active Power Filters. 2016 *International Symposium on Power Electronics, Electrical Drives, Automation and Motion* (*SPEEDAM*), Capri, 22-24 June 2016, 825-830. https://doi.org/10.1109/speedam.2016.7525899

[15] Yang, F., Bai, W., Huang, X., Wang, Y., Liu, J. and Kang, Z. (2024) Slow-Scale Bifurcation Analysis of a Single-Phase Voltage Source Full-Bridge Inverter with an LCL Filter. *Energies*, **17**, Article 4168. https://doi.org/10.3390/en17164168

[16] Büyük, M., Tan, A., Tümay, M. and Bayındır, K.Ç. (2016) Topologies, Generalized Designs, Passive and Active Damping Methods of Switching Ripple Filters for Voltage Source Inverter: A Comprehensive Review. *Renewable and Sustainable Energy Reviews*, **62**, 46-69. https://doi.org/10.1016/j.rser.2016.04.006

Nomenclature

L_{mini}/L_{maxi}	minimum/maximum filter inductance
K	LCL filter inductance sharing coefficient
S_N	apparent power of the AC load
U_{ph}	voltage between phases on the AC load
SPWM	Sinusoidal Pulse-Width-Modulation
THDu/I	Total Harmonic distorsion for voltage or current
I_n	rated current in the AC load
C_{mini}/C_{maxi}	minimum/maximum filter capacitor capacity